

Proceedings of the European Conference Physics of Magnetism 2011 (PM'11), Poznań, June 27–July 1, 2011

Exchange Bias in Ni–Mn–Sn Heusler Alloy Films

I. GOŚCIAŃSKA^a, K. ZAŁĘSKI^b, H. GŁOWIŃSKI^b, YU.V. KUDRYAVTSEV^c
AND J. DUBOWIK^b

^aDepartment of Physics, A. Mickiewicz University, Umultowska 85, 61-614 Poznań, Poland

^bInstitute of Molecular Physics, PAS, M. Smoluchowskiego 17, 60-179 Poznań, Poland

^cInstitute of Metal Physics, NANU, Vernadsky Ave. 36, Kiev-142, Ukraine

We report a relatively large exchange bias effect observed for the first time in Ni–Mn–Sn thin films with different microstructure and composition: a Ni₅₀Mn₃₆Sn₁₄ epitaxial film (A), a Ni₅₀Mn₄₃Sn₇ film which is phase decomposed (B), and a NiMn/Ni₅₀Mn₂₅Sn₂₅ bilayer (C). Despite the samples differ markedly in both microstructure and composition H_{EB} does not substantially differ at 5 K. Exchange bias decreases with increasing T approximately as $H_{EB}(T) \propto H_{EB}(5\text{ K})/T$ with $H_{EB}(5\text{ K})$ of 180 Oe and 60 Oe for sample B and C, respectively and almost linearly for sample A with $H_{EB}(5\text{ K}) = 65\text{ Oe}$. Blocking temperature where the exchange bias vanishes is 40, 50 and 80 K for sample A, C and B, respectively. The results suggest that the role of AFM/FM interfaces is not substantial in formation of exchange bias in Ni–Mn–Sn Heusler alloy films and exchange bias is rather related to AFM/FM interactions in nanoscale.

PACS: 75.70.Ak, 75.30.Et

1. Introduction

In conventional ferromagnetic/antiferromagnetic (FM/AFM) systems involving a FM/AFM interface the role of the AFM layer is to provide at the interface a net magnetization which is irreversible during reversal of the FM magnetization, resulting in a shift of the hysteresis loop. EB has been observed in NiMn-based Heusler bulk alloys NiMnSn [1]. The effect could be simply understood as resulting from the exchange anisotropy created at the interface between AFM and FM that exist in a martensite phase. Antiferromagnetic correlations have been recently identified by neutron polarization analysis [2]. In a more detailed study [3] it has been shown that the Ni–Mn–Sn can be identified as a reentrant spin glass (SG) with both ferromagnetic and glassy phases coexisting together at low temperatures in the field-cooled state. The observed exchange pinning has been interpreted in terms of the onset of spin glass freezing below the blocking temperature of 80 K.

To sum up, the EB in some off-stoichiometric Heusler alloys results from the presence of a nonferromagnetic phase (AFM or SG) in otherwise FM alloy but understanding of its origin is far to be complete. For example, recently it has been shown that a large EB can be created in bulk NiMnIn [4] even after zero-field-cooling (ZFC) due to isothermal magnetization process. Such phenomenon has been attributed to a superferromagnetic unidirectional anisotropy formed during the initial magnetization process below a blocking temperature.

The aim of the present contribution is to show for the first time the behavior of EB in Ni–Mn–Sn thin films with miscellaneous microstructures resulting either from deposition or post annealing process (an epitaxial film, a film

with phase separation, a FM/AFM bilayer). Only thin film technology offers possibilities to produce such diverse microstructures. We anticipated that various microstructures of Ni–Mn–Sn films should result in markedly different EB effects.

2. Experimental and results

The thin film structures prepared by magnetron sputtering comprise: a MgO/Ni₅₀Mn₃₆Sn₁₄(500 nm) off-stoichiometric epitaxial film with clearly visible martensitic transformation at $T \approx 125\text{ K}$ (sample A), a Si/Ni₅₀Mn₄₃Sn₇(100 nm) film phase decomposed into antiferromagnetic (AFM) NiMn and ferromagnetic (FM) Ni–Mn–Sn (sample B), and a Si/NiMn(50 nm)/Ni₅₀Mn₂₅Sn₂₅(30 nm) bilayer with an AFM/FM interface but with no EB near room temperature (sample C). The films were deposited on single crystalline MgO(001) or Si(100) substrates by means of cosputtering from Ni, MnNi and MnSn targets at 350°C. Base pressure was better than 2×10^{-7} Torr and Ar pressure was 8 mTorr. For sample C the thermal annealing was performed at temperature T_a of 300°C in 10^{-6} Torr up to several hours. Structural characterization of the films was performed by X-ray diffraction (XRD) with Co K_α radiation. Magnetization measurements were carried out by Physical Property Measuring System (PPMS).

The results of structural characterization are shown in Fig. 1. Figure 1a shows θ – 2θ scan of XRD for the film A. The (002) and (004) reflections of Ni₅₀Mn₃₆Sn₁₄ are only observed due to its epitaxial growth on MgO(100). Lattice constant of $a = 0.605\text{ nm}$ estimated from these peaks was nearly equal to the reported value [5] for bulk alloy. A ϕ scan (not shown)

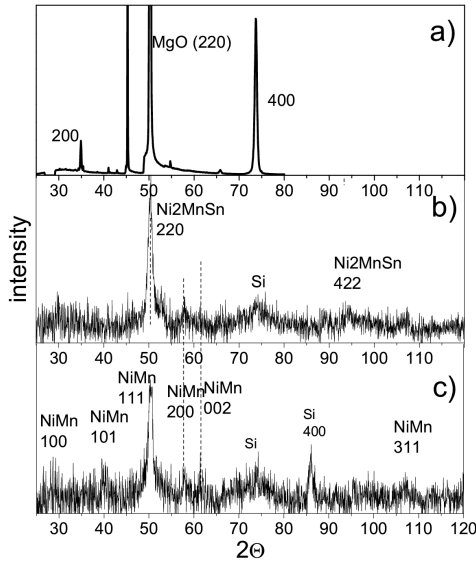


Fig. 1. X-ray diffraction patterns of a $\text{Ni}_{50}\text{Mn}_{36}\text{Sn}_{14}$ epitaxial film on a MgO substrate (a) and a $\text{Ni}_{50}\text{Mn}_{43}\text{Sn}_7$ on a Si substrate (b). Part (c) shows XRD pattern of a NiMn film on a Si substrate.

of the reflection from the (200) planes for the epitaxial Ni–Mn–Sn film reveals shift of 45° from those for (200) peaks of the MgO substrate. From these data, the epitaxial relationship for the films was confirmed to be $\text{Ni}_{50}\text{Mn}_{36}\text{Sn}_{14}(001)[100]//\text{MgO}(001)[110]$. Intensity ratio of (002) to (004) peak is of 0.08 which suggests that the structural quality of the epitaxial film *A* is high but with some Ni atoms replaced by Mn.

Figure 1b shows XRD of the polycrystalline film *B* deposited on Si(100) at 350°C . For XRD θ – 2θ scans the samples deposited on Si were tilted of 1 – 15° with respect to a diffractometer stage to get rid of a very strong (400)Si reflection but some diffused reflection between 70 – 80° is still seen. Most reflections can be ascribed to NiMn ordered phase. XRD of a reference polycrystalline NiMn film deposited on a (100)Si substrate is shown in Fig. 1c for comparison. The presence of reflections (220) and (422) from $B2$ (or $L2_1$) Heusler alloy structure are also seen in Fig. 1b. Their presence clearly support that some amount of Ni–Mn–Sn (of 10–20%) remains in the film *B* and confirms its phase separation on AFM NiMn with $L1_0$ structure and Ni–Mn–Sn with the Heusler alloy structure. Furthermore, additional magnetization measurements of sample *B* suggest that the phase separated Ni–Mn–Sn has composition not far from stoichiometric Ni–Mn–Sn Heusler alloy. Such observation is in agreement with that recently reported by Yuhasz et al. [6] in bulk $\text{Ni}_{50}\text{Mn}_{39}\text{Sn}_{11}$.

Figure 2 shows hysteresis loops taken at 5 K for samples *A*, *B*, and *C*, respectively. Since coercivity in the films differs much (see Fig. 3), the loops are shown in normalized scale H/H^- , where H^- is the “left” switching field of a given sample. The exchange bias field

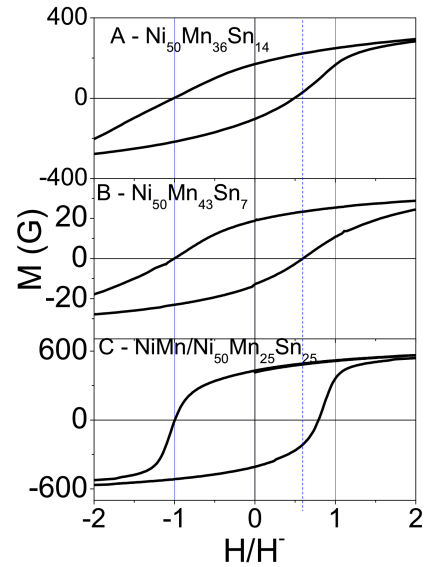


Fig. 2. Hysteresis loops of Ni–Mn–Sn films taken at 5 K: $\text{Ni}_{50}\text{Mn}_{36}\text{Sn}_{14}$ — *A*, $\text{Ni}_{50}\text{Mn}_{43}\text{Sn}_7$ — *B*, and NiMn/ $\text{Ni}_{50}\text{Mn}_{25}\text{Sn}_{25}$ bilayer — *C* films.

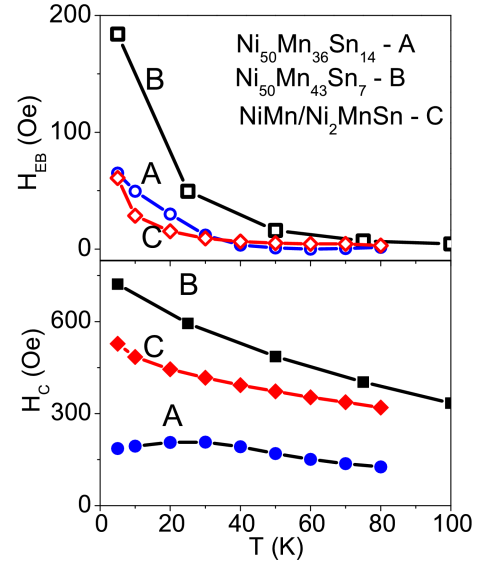


Fig. 3. (upper part) Temperature dependence of EB field for $\text{Ni}_{50}\text{Mn}_{36}\text{Sn}_{14}$ — *A*, $\text{Ni}_{50}\text{Mn}_{43}\text{Sn}_7$ — *B*, and NiMn/ $\text{Ni}_{50}\text{Mn}_{25}\text{Sn}_{25}$ bilayer — *C* films. (bottom part) Temperature dependence of coercive field for the same samples.

H_{EB} defined as $1/2(H^+ + H^-)$ amounts to $H_{\text{C}}^A/3 \approx 60$, $H_{\text{C}}^B/4 \approx 180$ and $H_{\text{C}}^C/8 \approx 65$ Oe for *A*, *B*, and *C*, respectively. It is worth noting that the shape of the loops of samples *A* and *B* are almost the same despite a large difference in H_{C} . The loops are much skewed and resembles those observed in bulk Ni–Mn–Sn alloys with EB [3, 4]. The skewing can be related to the presence of FM clusters embedded in a AFM matrix. On the other hand, the shape of the loop of sample *C* is typical for thin Heusler alloys film with the field applied along the easy

axis. The absolute values of the magnetization for the sample *B* differs significantly from that of the samples *A* and *C* (Fig. 2). While the saturation magnetization (M_S) at 5 K for *A* (in the martensitic phase) and *C* is of 450 and 650 G, respectively ($M_S = 700 \text{ G} - 4 \text{ mB/formula unit}$ is typical of well ordered stoichiometric $\text{Ni}_{50}\text{Mn}_{25}\text{Sn}_{25}$), the significantly lower value of M_S for sample *B* implies that the phase separation is high in the film and less than $\approx 10\text{--}20\%$ of its volume is occupied by FM phase depending on its dispersion. Temperature dependence of the magnetization of sample *B* (not shown) confirms the supposition that the composition of FM phase is not far from stoichiometric.

Figure 3 shows dependences of H_{EB} (upper part) and H_C (lower part) on temperature for our Ni–Mn–Sn thin film structures. The highest H_{EB} is for sample *B* with overdeveloped interfaces and amounts to $\approx 180 \text{ Oe}$ at 5 K, while H_{EB} are almost the same (65 and 60 Oe) for sample *A* and *B*, respectively. The main difference in $H_{EB}(T)$ for samples *A* and *B* (*C*) is that it almost linearly decreases with T and vanishes at $T_B = 40 \text{ K}$ for *A*, while for the samples *B* and *C* it varies roughly as $1/T$. The coercivity depends on temperature in a different way. The polycrystalline films *B* and *C* with substantially different AFM/FM interface contributions have the high values of H_C at 5 K of 750 and 500 Oe for sample *B* and *C*, respectively. Moreover, H_C monotonically decreases with T . On the contrary, the epitaxial film *A* has much lower H_C of 150–200 Oe and $H_C(T)$ has a broad but visible maximum at 30–40 K next to the blocking temperature of 40 K. This is nearly the same behavior as that observed for the bulk Ni–Mn–Sn alloys with reentrant spin-glass origin of EB [3, 4].

In spite of diverse microstructures in the investigated Ni–Mn–Sn films, a rough estimation of their relative interface surface (defined as $\sum_i S_i/V$, where the index i numbers individual entities of the FM phase of the mean surface S_i and V is the film volume) shows that their relative interface surfaces do not differ more than of one order. The highest value of the relative surface is for sample *B*. Nevertheless, the temperature characteristics of EB in sample *A* and *B*(*C*) differ substantially. Our preliminary interpretation of EB in the samples *B* and *C* is based on a domain state model [7] and assumes formation of a substantial composition gradient on the AFM/FM interfaces which leads to an increase of structural defects and to an increase in H_{EB} in result. In particular, the effect is most pronounced in the sample *B* with phase separation.

3. Conclusions

Exchange bias (EB) is normally observed in conventional systems (e.g. AFM/FM bilayers) with an interface between AFM/FM phases after field cooling. No conventional EB was observed in RT at NiMn/Ni₅₀Mn₂₅Sn₂₅ bilayers since the Néel temperature T_N of NiMn of 1070 K is much higher than the Curie temperature of Ni₅₀Mn₂₅Sn₂₅ of 330 K. However, we observed EB at low temperature region ($5 < T < 80 \text{ K}$) in Ni–Mn–Sn thin films with different microstructures. While EB observed in homogeneous film can be reasonably explained as originating from reentrant-spin-glass state, the same as that observed in bulk off-stoichiometric Ni₅₀Mn₃₄Sn₁₆[3], the exchange pinning in the heterogeneous film (*B*) or the film *C* with one AFM/FM interface has presumably a different origin. We tentatively connect EB in these samples to a high compositional gradient at the interfaces and hence to the presence of distributed FM and AFM couplings due to a high heterogeneity in nanoscale.

Acknowledgments

The financial support from MNiSW grant No. 733/N-DAAD is gratefully acknowledged.

References

- [1] Zhe Li, J. Chen, S. Yuan, S. Cao, J. Zhang, *Appl. Phys. Lett.* **91**, 112505 (2007).
- [2] S. Aksoy, M. Acet, P.P. Deen, L. Manosa, A. Planes, *Phys. Rev. B* **79**, 212401 (2009).
- [3] S. Chatterjee, S. Gori, S.K. De, S. Majumdar, *Phys. Rev. B* **79**, 092410 (2009).
- [4] B.M. Wang, Y. Liu, P. Ren, B. Xia, K.B. Ruan, J.B. Yi, J. Ding, X.G. Li, L. Wang, *Phys. Lett.* **106**, 077203 (2011).
- [5] T. Krenke, M. Acet, E.F. Wassermann, X. Moya, L. Manosa, A. Planes, *Phys. Rev. B* **72**, 014412 (2005).
- [6] W.M. Yuhasz, D.L. Schlagel, Q. Xing, K.W. Denis, R.W. McCallum, T.A. Lograsso, *J. Appl. Phys.* **105**, 07A921 (2009).
- [7] J. Keller, P. Miltényi, B. Beshoten, G. Güntherodt, U. Nowak, K.D. Usadel, *Phys. Rev. B* **66**, 11431 (2002).